Journal of Zhejiang University-SCIENCE A in press
www.jzus.zju.edu.cn; www.springer.com/journal/11582
E-mail: jzus_a@zju.edu.cn

Research Article
https://doi.org/10.1631/jzus.A2500241

A novel phosphazene-based flame retardant for dicyclopentadiene phenol epoxy resin: synthesis and performance evaluation

Yuyao JIA[1,2], Hao ZHU[1,2], Sheng ZOU[1], Wei BAI[1]✉, Qingyin WANG[1]

[1]*Chengdu Institute of Organic Chemistry, Chinese Academy of Sciences, Chengdu 610041, China*
[2]*University of Chinese Academy of Sciences, Beijing 101400, China*

Abstract: A novel high-melting-point phosphazene derivative, hexa(p-methylbenzamidephenoxy)cyclotriphosphazene (HBPCP), was designed and synthesized in this work. The goal is to address the inherent flammability of dicyclopentadiene phenol epoxy resin (EP) and the limitations of conventional phosphazene flame retardants—such as hexa phenoxy cyclotriphosphazene (HPCP)—which suffer from poor thermal stability and processing-related migration. The HBPCP was synthesized through a three-step process—nucleophilic substitution, oxidation, and acylation-amidation—with overall yields ranging from 89% to 95%. HBPCP remains solid at the EP processing temperature (185 °C), effectively preventing additive migration and subsequent degradation of mechanical properties. Thermogravimetric analysis (TGA) revealed that HBPCP exhibits excellent thermal stability, with a residual char yield of 41.82% at 800 °C. Moreover, flame retardancy tests showed that adding 12.5 wt% HBPCP increased the limiting oxygen index (LOI) of EP from 21.19% to 27.13%, and resulted in a UL-94 V-0 rating. Additionally, the peak heat release rate (PHRR) and total smoke production (TSP) were reduced by 49.2% and 41.8%, respectively, as compared to neat EP. In terms of mechanical performance, EP/HBPCP-5 showed a 14.6% improvement in tensile strength compared to neat EP. Even for higher loadings upon the HBPCP samples, the mechanical properties remained superior to those of the unmodified resin. Furthermore, HBPCP incorporation increased the free volume in the EP matrix, reducing both the dielectric constant (D_k) and dielectric loss (D_f) at high frequencies. At 10 GHz, the dielectric constant decreased from 3.26 to 3.10, thus meeting requirements for low-dielectric electronics applications. Overall, this study provides an effective method to create high-performance epoxy resins with enhanced flame retardancy, improved mechanical properties, and low dielectric characteristics.

Key words: Cyclic triphosphazene derivatives; Flame retardant; Epoxy resin; High thermal stability; Low dielectric constant; Electronics materials

1 Introduction

Epoxy resin (EP) is a widely used thermosetting polymer, primarily employed in functional coatings, adhesives, electrical insulation and encapsulation, sporting goods, and the aerospace industry (Zhang et al., 2016; Xu et al., 2018; Hu et al., 2020; Wang et al., 2016). Dicyclopentadiene (DCPD) phenol epoxy resin, which is synthesized using dicyclopentadiene and phenol as the primary framework, has the advantages of alicyclic epoxy resins—excellent electrical properties, low viscosity, high adhesion, good heat resistance, and strong acid/alkali resistance. Moreover, it significantly improves heat resistance and reduces water absorption due to its rigid benzene ring structures. The performance of DCPD surpasses that of conventional epoxy resins, meeting the stringent requirements for heat resistance, acid/alkali resistance, low water absorption, low thermal expansion coefficient, low shrinkage, and low internal stress in electrical encapsulation applications. It serves as a key raw material for producing semiconductor encapsulation compounds (Fu et al., 2024) and is also employed in laminate production (Lu et al., 2023). However, EP exhibits a low limiting oxygen index (LOI) of

✉ Wei BAI, baiwei@cioc.ac.cn
Yuyao JIA, https://orcid.org/0009-0001-4795-3664
Wei BAI, https://orcid.org/0000-0003-1705-8738

Received June 8, 2025; Revision accepted Oct. 11, 2025; Crosschecked

© Zhejiang University Press 2025

Unedited

approximately 21.0%, as well as poor self-extinguishing properties. It also releases substantial amounts of heat and toxic smoke during combustion, posing significant threats to health and property, and compromising urban fire safety (Müller and Schartel, 2016; Jin et al., 2019; Müller et al., 2016). Therefore, developing efficient flame retardants to produce flame-retardant EP thermosetting materials remains an urgent challenge.

Traditionally, halogen-containing flame retardants have been widely employed in EP systems due to their excellent flame-retarding efficiency. However, halogenated flame retardants release toxic gases and substantial amounts of smoke during combustion, posing significant environmental and health hazards (Liu et al., 2019; Zhu et al., 2019). As a result, the use of halogenated flame retardants is being increasingly restricted. Phosphorus-based flame retardants decompose at relatively low temperatures, generating compounds such as phosphoric and metaphosphoric acid. These acidic species catalyze the dehydration and charring of polymers, promoting the formation of a dense char layer on the polymer surface; this acts as a barrier to oxygen and heat, thereby retarding combustion (Cheng et al., 2024; Wang et al., 2024). Nitrogen-based flame retardants, upon decomposition, release non-combustible gases that dilute the oxygen concentration and reduce the generation of flammable volatiles (Yang et al., 2025; Li et al., 2025).

Since nitrogen-containing compounds mainly function in the gas phase, they are often used in combination with other flame retardants. For instance, phosphorus-nitrogen flame retardants, which incorporate both phosphorus (P) and nitrogen (N), exhibit synergistic flame-retardant effects in both the gas and condensed phases. Moreover, being halogen-free, they have attracted significant research interest (Chen et al., 2025; Wei et al., 2016). Among them, phosphazene compounds, which consist of alternating –N=P– bonds, are rich in both nitrogen and phosphorus (Huo et al., 2021). They are generally categorized into two main types: cyclophosphazenes and polyphosphazenes. Polyphosphazenes are inherently flame-retardant polymeric materials with flexible backbones, and are commonly used as high-temperature elastomers (Liu et al., 2020). Cyclophosphazenes possess a conjugated structure analogous to benzene rings, which endows them with high thermal stability. Furthermore, their high nitrogen and phosphorus content imparts excellent flame retardancy, while their favorable dielectric properties make them suitable for low-dielectric epoxy resin applications (Bose et al., 2010).

Hexaphenoxycyclotriphosphazene (HPCP) is a phosphorus-nitrogen flame retardant that is commonly used in epoxy resin systems. However, it induces a plasticization effect which reduces the rigidity of the epoxy matrix (Khalidah et al., 2021). During the processing of dicyclopentadiene phenol epoxy resin (DCPD-EP) into laminates, high processing temperatures present additional challenges. Due to its low melting point of 112 °C, HPCP tends to migrate toward the material surface under heat and pressure during processing. This leads to an uneven distribution of the flame retardant within the polymer matrix, ultimately degrading the mechanical properties of the resulting composites (Jiang, 2022). Additionally, its thermal stability is relatively poor, with a char residue of only 1.6% at 800 °C (Tang et al., 2010). To address these limitations, Shin et al. (2009) synthesized three phosphazene derivatives—HPCTP, CTCP, and HNCP—through reactions of hexachlorocyclotriphosphazene with phenol, catechol, and 2,3-dihydroxynaphthalene, respectively. These derivatives were subsequently incorporated into ABS resin at mass loadings of 10%, 15%, and 20%. At a 20 wt% loading and at 5% mass loss ($T_{5\%}$), the HNCP/ABS composite exhibited a significant increase in the temperature, from 275 °C to 375 °C, in the tensile strength from 294 kg/cm² to 322 kg/cm², and in the elongation at the break from 8.8% to 10.9%, as compared to the HPCTP/ABS system. Its UL-94 rating improved from V-2 to V-1, and the limiting oxygen index (LOI) increased from 22.2% to 24.9%. Meanwhile, the incorporation of the naphthalene ring significantly enhanced the thermal stability, mechanical properties, and flame retardancy of the HNCP/ABS composite.

In order to mitigate the adverse impact of flame retardants on the mechanical properties of polymer

Unedited

materials, Atika et al. (2023) synthesized a series of hexasubstituted cyclotriphosphazene derivatives with varying terminal alkyl chain lengths (pentyl, nonyl, and decyl). These derivatives achieved LOI values as high as 26.28% for the nonyl and decyl-substituted compounds, and 25.71% for the pentyl-substituted derivatives. Furthermore, the influence of terminal alkyl chain length on the mechanical properties was investigated in their study. The addition of methylene groups within the alkyl chains led to a dilution effect: the Young's modulus decreased from 156.36 MPa for the pentyl derivative to 99.30 MPa for the decyl derivative, though this was still higher than that of neat EP (58.55 MPa). Therefore, these flame retardants not only improved the flame retardancy of EP but also enhanced its mechanical performance. The melting point of a compound is primarily governed by intermolecular interactions; stronger intermolecular forces result in higher melting points (Chen et al., 2024). Modifying HPCP via nucleophilic substitution with bulky substituents, such as naphthol or biphenyl monophenol, often results in extremely low yields of the target product and difficulties in purification due to substantial steric hindrance.

In this study, a novel phosphazene derivative, hexa (p-methylbenzamidophenoxy)cyclotriphosphazene (HBPCP), which is characterized by a high melting point and excellent thermal stability, was synthesized through a stepwise introduction of benzene rings. This two-step strategy for incorporating benzene rings significantly enhanced the yield of the target product while producing virtually zero byproducts. The amide linkage effectively connects the two benzene rings, and the relatively low nucleophilicity of the amide nitrogen prevents premature curing of the epoxy resin during processing. Additionally, the nitrogen in the amide group plays a crucial role in flame retardancy. Incorporating HBPCP into the epoxy resin matrix led to the formation of EP/HBPCP composites that exhibit enhanced flame retardant properties. Moreover, HBPCP remained solid at the 185 °C processing temperature of the epoxy resin, addressing the issue of mechanical property degradation that is commonly associated with migration of phosphazene flame retardants. Moreover, the incorporation of the bulky and stable HBPCP particles increased the free volume within the resin, resulting in a slight reduction in its dielectric constant. This is particularly beneficial for applications requiring both flame retardancy and low dielectric epoxy resins.

2 Materials and methods

2.1 Materials

Hexachlorocyclotriphosphazene (HCTP, 99%), p-hydroxybenzaldehyde (99%), K_2CO_3 (99%) $KMnO_4$ (99%), NaOH (99%), $SOCl_2$ (99%), H_2SO_4 (95-98%), tetrahydrofuran (THF, AR), N,N-Dimethylformamide (DMF, AR), ethyl acetate (AR), p-toluidine (99%), triethylamine (99%), 4,4′-diaminodiphenyl sulfone (DDS, 99%), and a dicyclopentadiene-based epoxy resin (EP) with an epoxy equivalent weight of 278.3 g/eq were purchased from Hunan Shengjiade Chemical Co., Ltd.

2.2 Synthesis of Hexa(p-formylphenoxy)cyclotriphosphazene (HAPCP)

A mixture of p-hydroxybenzaldehyde (5.13 g, 42 mmol), anhydrous K_2CO_3 (5.8 g, 42 mmol), and tetrahydrofuran (THF, 80 mL) was added to a 250 mL oven-dried three-necked flask and stirred at room temperature. Hexachlorocyclotriphosphazene (2.08 g, 6 mmol) was dissolved in THF (40 mL) and added with a dropper to the reaction flask over the course of 30 minutes. The resulting mixture was then heated to 65 °C and stirred for 24 hours. Upon completion, the reaction mixture was concentrated through rotary evaporation. The crude product was washed twice with distilled water and once with ethyl acetate to obtain a solid white product (HAPCP, 4.7 g), with a yield of 91%.

2.3 Synthesis of Hexa(p-carboxyphenoxy)cyclotriphosphazene (HCPCP)

HAPCP (5.17 g, 6 mmol), NaOH (1.82 g, 45.5 mmol), distilled water (30 mL), and THF (50 mL) were added to a 250 mL beaker and stirred at room temperature. $KMnO_4$ (8.71 g, 55 mmol) was divided into several portions and added gradually to the reaction mixture until its purple color completely

Unedited

disappeared. After completion, the THF was removed under reduced pressure. The resulting mixture was vacuum filtered and acidified, then dried at 80 °C for 12 hours to obtain a white solid product, HCPCP (5.11 g), with a yield of 89%.

2.4 Synthesis of Hexa(p-methylbenzamidophenoxy)cyclotriphosphazene (HBPCP)

HCPCP (5.75 g, 6 mmol) was added to a 100 mL round-bottom flask equipped with a reflux condenser and a gas absorption apparatus. Thionyl chloride (11.9 g, 100 mmol) and 3–5 drops of N,N-dimethylformamide (DMF) as a catalyst were then introduced. The mixture was refluxed at 65 °C for 24 hours under stirring. Following completion, the excess thionyl chloride was removed, yielding a white powder intermediate.

Subsequently, p-toluidine (4.5 g, 42 mmol) and triethylamine (4.3 g, 42 mmol) were dissolved in 70 mL of THF, while the intermediate was dissolved in 210 mL of THF. The solution of the intermediate was added dropwise into a three-neck flask over 30 minutes in ice-bath conditions, which was followed by stirring for 6 hours. The reaction mixture was then washed twice with 1 mol/L K_2CO_3 solution and once with ethyl acetate. The final product was dried at 70 °C for 2 hours to obtain a white powder (8.5 g), with a yield of 95%.

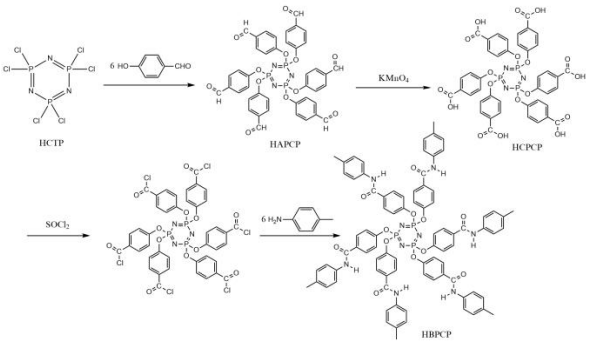

Fig. 1 Scheme for the synthesis of Hexa(p-methylbenzamidophenoxy)cyclotriphosphazene (HBPCP)

2.5 Preparation of EP/HBPCP composites

HBPCP was ground in a pulverizer and passed through a 200-mesh sieve. Then, 100 g of DPNE and the specified amount of HBPCP were degassed in a vacuum at 185 °C. Next, 22 g of DDS was incorporated into the epoxy resin, and the mixture was blended in a vacuum at 185 °C for 5 min. The homogenized blend was poured into a steel mold and cured at 135 °C for 3 h, followed by post-curing at 185 °C for 2 h to yield the target EP/HBPCP samples. The details of the prepared EP samples are summarized in Table 1.

Table 1 Preparation data of the HBPCP/EP composites

Sample	EP (g)	DDS (g)	HBPCP (g)	HBPCP content (wt%)
EP	100	22	0	0
EP/HBPCP-1	100	22	1.24	1
EP/HBPCP-5	100	22	6.4	5
EP/HBPCP-10	100	22	13.6	10
EP/HBPCP-12.5	100	22	17.6	12.5

2.6 Characterization methods

Fourier-transform infrared (FTIR) spectroscopy was performed using a Thermo Fisher Nicolet 670 (Thermo Fisher Scientific USA) spectrometer in the range of 4000~500 cm^{-1} with a resolution of 4 cm^{-1}. The samples were homogenized with KBr and pressed into pellets prior to analysis.

^{1}H NMR and ^{31}P NMR spectra were acquired at ambient temperature on a Bruker AVANCE 400 MHz spectrometer using deuterated dimethyl sulfoxide (DMSO-d_6) as the solvent.

Differential scanning calorimetry (DSC) was performed with a TA DSC2500 (TA Instruments USA) instrument to determine the phase transition temperatures of HBPCP. Measurements were conducted in a nitrogen atmosphere with a heating rate of 10 °C·min^{-1} from 25 °C to 300 °C.

Thermogravimetric analysis (TGA) was carried out using a Netzsch STA 449 F3 (NETZSCH GER) analyzer. The samples (8~10 mg) were loaded into

Unedited

platinum crucibles and heated from ambient temperature to 800 °C at 10 °C·min^{-1} under nitrogen air flow.

Limiting oxygen index (LOI) values were measured according to ASTM D2863 on an FTT0077 (UK) oxygen index tester. The specimen dimensions were 80 × 10 × 4 mm^3.

Vertical burning tests (UL-94) were conducted using an FTT0082 (UK) apparatus with specimens of size 80 × 10 × 4 mm^3.

Cone calorimetry was performed following ISO 5660 utilizing a VOUCH 6810 instrument (Yangyi Wolun, Suzhou) at a radiant flux of 50 kW/m^2. The specimens (dimensions: 100 × 100 × 3 mm^3) were wrapped in aluminum foil for the testing.

Scanning electron microscopy (SEM) micrographs of char residues from EP and EP/HBPCP composites were acquired using a ZEISS GeminiSEM 300 (GER) microscope at 15 kV acceleration voltage. The instrument was coupled with energy-dispersive X-ray spectroscopy (EDS) for elemental mapping.

Tensile properties were evaluated as per ASTM D 638-2010 using a universal testing machine (Instron 4302 USA) at ambient temperature. Dumbbell-shaped specimens (dimensions: 250 × 50 × 2 mm^3) were tested, with the values recorded being averages of five measurements.

The specimens were molded using an electric vulcanization press (SY-6210-A China) under controlled thermal compression.

The measurements were performed/carried out using a Keysight Technologies P9373A network analyzer and a QWED SPDR fixture at a frequency of 10 GHz.

3 Results and discussion

3.1 Characterization of HBPCP

The synthesized product, HBPCP, was structurally characterized using Fourier-transform infrared (FTIR) and nuclear magnetic resonance (NMR) spectroscopy. According to the FTIR spectrum (Fig. 2), the absorption peak at 1711 cm^{-1} corresponds to the C=O stretching vibration of aldehyde (–CHO) and carboxylic acid (–COOH) groups; the peak at 1650 cm^{-1} corresponds to the C=O stretching vibration of amide bonds (–CONH–). Additionally, the peaks at 2824 cm^{-1} and 2727 cm^{-1} represent the C–H stretching vibrations of aldehyde groups. The absorption peaks between 3300 and 2500 cm^{-1} correspond to the O–H stretching vibrations of carboxylic acid groups. And the absorption peaks between 3500 and 3100 cm^{-1} represent the N–H stretching vibrations of amide bonds (Chen et al., 2024).

The ^{1}H and ^{31}P NMR spectra of HBPCP are presented in Figs. 3a and 3b, respectively. In the ^{1}H NMR spectrum, the signal at 2.28 ppm corresponds to the methyl protons (–CH_3) of the p-methylbenzamide substituents. The signal at 10.12 ppm is attributed to the amide proton (–NH–). Meanwhile, the multiplet between 7.08 and 7.93 ppm corresponds to aromatic protons. The ^{31}P NMR spectrum (Fig. 2b) displays a single sharp peak at 7.59 ppm, indicating that all phosphorus atoms in the cyclotriphosphazene ring experience equivalent chemical environments; this is consistent with a symmetrical substitution pattern. These spectroscopic results confirm the successful synthesis of HBPCP with the intended molecular architecture (Chen et al., 2024; Wang et al., 2015).

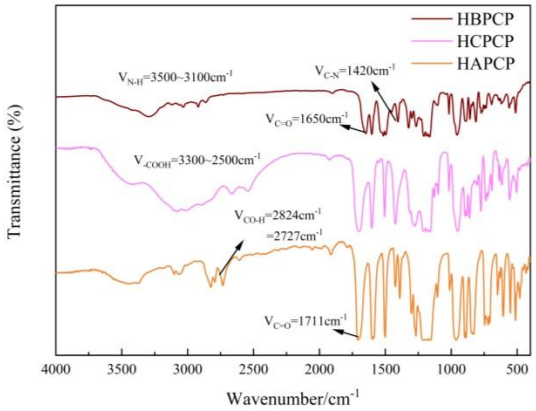

Fig. 2 FTIR spectra of HAPCP, HCPCP, and HBPCP

Unedited

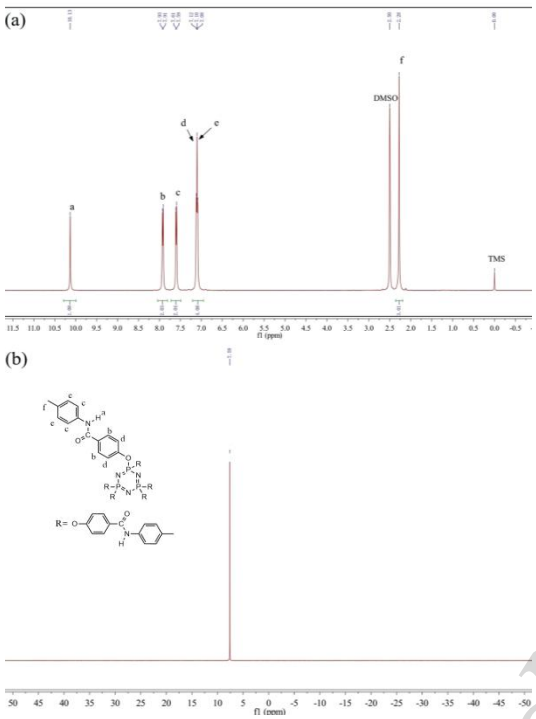

Fig. 3 (a) ^{1}H NMR spectra of HBPCP, (b) ^{31}P NMR spectra of HBPCP

3.2 Thermal stability

The thermogravimetric (TGA) and derivative thermogravimetric (DTG) curves of HBPCP and EP/HBPCP composites are presented in Fig. 4. Key thermal decomposition parameters—including the 5% weight-loss temperature ($T_{5\%}$), the maximum decomposition-rate temperature (T_{max}), and the char residue at 800 °C—are summarized in Table 2. As shown in Fig. 4b, HBPCP exhibits two weight-loss stages, which correspond to two DTG peaks. The first stage occurs between 330 °C and 407 °C, and corresponds to a DTG peak at 364 °C (T_{max1}) with a weight loss of 39%. This stage coincides with the decomposition of ether bonds, amide linkages, and methyl groups. The second stage occurs between 407 °C and 434 °C, corresponding to a DTG peak at 419 °C (T_{max2}) with a weight loss of 4%. This stage coincides with the degradation of the cyclotriphosphazene backbone (Cheng et al., 2019). The char yield at 800 °C was 41.82%, indicating good charring performance. Hexaphenoxycyclotriphosphazene (Jiang et al., 2019) exhibits a melting point of just 114 °C and a char residue of only 1.2% at 800 °C. In contrast, Nabipour et al. (2022) synthesized a macromolecular cyclotriphosphazene derivative named hexa[(E)-4-{[(4H-1,2,4-triazol-4-yl)imino]methyl}-2-methoxyphenyl] cyclotriphosphazene (HHCTP) using 4-amino-4H-1,2,4-triazole and vanillin as raw materials. The 10% weight-loss temperature ($T_{10\%}$) was 275 °C. The maximum decomposition-rate temperature (T_{max}) was 300 °C, while the char yield at 800 °C was 29.9%. Compared to other phosphazene-based flame retardants, HBPCP exhibits superior thermal stability. Pure EP displays a char residue of 16.18% at 800 °C. With increasing HBPCP loading, the char residue gradually increases, and the experimentally measured values exceed the theoretical calculations, indicating that including HBPCP promotes the formation of carbon layers (Jiang et al., 2012). Under an N_2 atmosphere (Fig. 4b), both EP and EP/HBPCP composites display a single decomposition peak, indicating a single major weight-loss stage during thermal degradation. Pure EP exhibits the highest $T_{5\%}$ (382.9 °C) and T_{max} (424.1 °C). However, these parameters progressively decrease with increasing HBPCP content. This is because the phenoxy radicals and phosphorus-containing compounds generated during HBPCP decomposition accelerate degradation of the EP matrix. Phenoxy radicals, disproportionation products, and phosphorus oxides derived from high-temperature pyrolysis collectively quench gas-phase free radicals during combustion, as well as enhance char formation in the condensed phase. Additionally, premature HBPCP decomposition releases small non-combustible molecules, which further improves the flame retardancy (Sun et al., 2014).

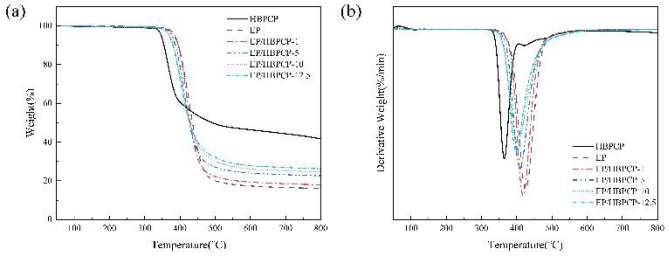

Fig. 4 (a) Thermogravimetric (TG) and (b) derivative TG (DTG) curves of HBPCP and EP/HBPCP composites under N_2 atmosphere

Unedited

Table 2 Data of TG and DTG for HBPCP and EP/HBPCP composites in N_2 atmosphere

Sample	T5% (°C)	Tmax1 (°C)	Tmax2 (°C)	Char yields at 800 °C (%)	
				Test values	Calculated values
HBPCP	346.7	364.2	419.8	41.82	—
EP	382.9	424.1	—	16.18	—
EP/HBPCP-1	385.1	417.2	—	18.03	16.44
EP/HBPCP-5	377.1	407.2	—	22.68	17.46
EP/HBPCP-10	369.5	399.6	—	24.68	18.74
EP/HBPCP-12.5	369.2	396.2	—	26.26	19.39

Next, Differential Scanning Calorimetry (DSC) analysis of HBPCP was performed. Analysis from ambient temperature to 300 °C revealed no distinct endothermic peaks. A gradual upward trend in the range of 300–350 °C corresponds to an endothermic event, which is consistent with the onset of HBPCP decomposition observed in TGA. This decomposition-related endothermic peak confirms that HBPCP exhibits no melting transitions before thermal degradation, and remains thermally stable below 300 °C. During epoxy processing at 185 °C, HBPCP retains its solid-state integrity, preventing migration to the epoxy surface under pressure and elevated temperature. This stability ensures uniform dispersion within the epoxy matrix, thereby preventing the degradation of mechanical properties caused by uneven distribution of additives.

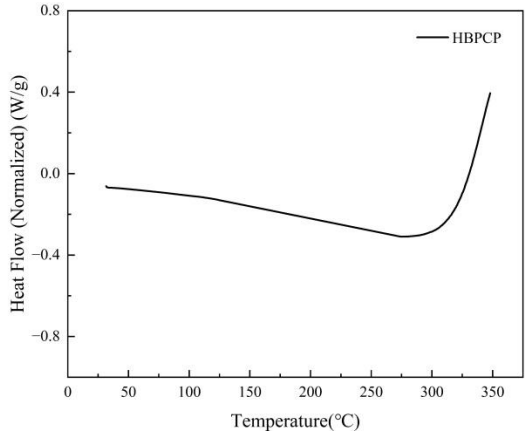

Fig. 5 DSC curves of HBPCP

3.3 Flame retardancy

3.3.1 LOI and UL-94 vertical burning tests

The flame retardancy of pure EP and EP/HBPCP composites was evaluated using the limiting oxygen index (LOI) and vertical burning (UL-94) tests. As shown in Table 3, the LOI value increased from 21.19% for pure EP to 27.13% for the EP/HBPCP-12.5 composite. Both EP/HBPCP-10 and EP/HBPCP-12.5 passed the UL-94 test and achieved a V-0 rating. No HBPCP-based sample exhibited dripping during combustion, confirming HBPCP's excellent anti-dripping effect within the EP matrix. The traditional phosphorus-nitrogen flame retardant ammonium polyphosphate (APP) is rich in phosphorus (P) and nitrogen (N). Elemental P exists in the form of polyphosphoric and metaphosphoric acids, which during combustion promote dehydration, cross-linking, and cyclization reactions, thereby facilitating the formation of a char layer. The elemental N acts as a flame retardant in the gas phase, generating and releasing large amounts of non-combustible gases such as ammonia, which dilutes oxygen and combustible small molecules. In contrast, the elemental P in the phosphazene skeleton of HBPCP can directly undergo cross-linking reactions with the epoxy resin matrix at high temperatures, forming bonds such as P–O–C. The resulting char layer exhibits high strength and excellent resistance to oxidation. Besides functioning as a gas-phase flame retardant, the elemental N in HBPCP—through the cleavage and rearrangement of amide bonds—promotes cross-linking within the epoxy resin molecules, thereby enhancing carbonization. Furthermore, its abundant benzene ring structures improve the stability of the char layer. (Seraji et al., 2021).

Table 3 LOI and UL-94 vertical burning test results

Unedited

for EP and EP/HBPCP composites

Sample	LOI (%)	UL-94		
		t_1/t_2 (s)	Dripping	Rating
EP	21.19	165/0	Yes	NR
EP/HBPCP-1	22.44	109/2	No	NR
EP/HBPCP-5	23.55	19/7	No	V-1
EP/HBPCP-10	24.9	7/3	No	V-0
EP/HBPCP-12.5	27.13	1/6	No	V-0

3.3.2 Cone calorimeter test

To further compare the flame retardancy of pure EP and EP/HBPCP composites, cone calorimetry tests were conducted to evaluate four combustion parameters—heat release rate (HRR), total heat release (THR), total smoke production (TSP), and smoke production rate (SPR). The results are summarized in Table 4. Without flame retardants, pure EP released a large amount of heat during combustion, with a peak heat release rate (PHRR) of 1,314.31 kW/m² and a THR of 111.78 MJ/m². As the HBPCP content increased, both PHRR and THR progressively decreased, indicating improved flame retardancy. These findings are consistent with the LOI and UL-94 test results.

According to Kurta et al. (2013), 60%–80% of fire-related fatalities result from excessive smoke inhalation. Therefore, smoke suppression is a critical factor in fire safety evaluation. Fig. 5c and 5d show the total smoke production (TSP) and smoke production rate (SPR) curves. More details on the data are given in Table 4. As HBPCP content increased, both the TSP and peak SPR (PSPR) values gradually decreased. Specifically, at 10 wt.% HBPCP loading, TSP decreased by 41.76% and PSPR decreased by 26.09%. However, at 12.5 wt.% loading, both TSP and PSPR increased slightly. This may be attributed to incomplete combustion as caused by the addition of excessive HBPCP. This is supported by the significantly reduced CO and CO_2 emissions, as shown in Table 4. Furthermore, HBPCP incorporation significantly suppressed emissions of toxic gases such as CO and CO_2, confirming its excellent inhibition of smoke and gas.

The fire growth index (FGI) and the fire performance index (FPI) are key parameters derived from cone calorimetry which are commonly used to evaluate material flame retardancy. FGI is defined as the ratio of the peak heat release rate (PHRR) to the time to reach PHRR (t-PHRR); a higher FGI indicates faster fire propagation (Li et al., 2018; Yuan et al., 2018). Fig. 6e shows that the FGI of the composites decreases as HBPCP content increases. FPI is defined as the ratio of time to ignition (TTI) to PHRR, and is correlated with large-scale fire performance under realistic fire conditions. FPI is inversely related to the level of fire hazard. Moreover, lower FPI values imply a more rapid onset of flashover (Wang et al., 2019). Fig. 6f shows that FPI values increase with the addition of HBPCP, confirming HBPCP's significant potential to reduce the fire risk of EP-based materials.

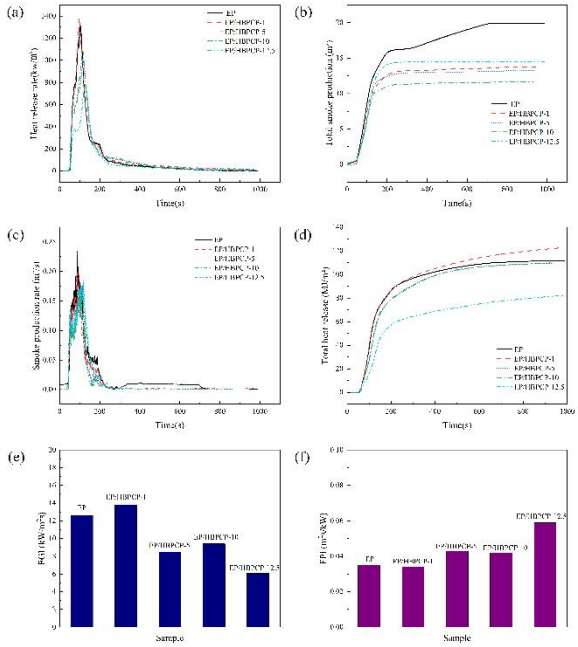

Fig. 6 (a) HRR curves, (b) THR curves, (c) SPR curves, (d) TSP curves, (e) FGI, (f) FPI of EP and EP/HBPCP composites

Table 4 The cone calorimeter results for the EP and EP/HBPCP composites

Sample	THR (MJ/m²)	PHRR (kW/m2)	TSP (m²)	PSPR (m²/s)	ACOY(kg/kg)	ACO_2Y(kg/kg)
EP	111.78	1314.31	19.94	0.23	0.54	6.64
EP/HBPCP-1	122.48	1380.38	13.81	0.19	0.46	5.13

Unedited

EP/HBPCP-5	109.68	997.07	13.23	0.18	0.51	6.01
EP/HBPCP-10	109.78	1087.01	11.63	0.17	0.51	6.09
EP/HBPCP-12.5	83.99	757.29	14.48	0.18	0.43	4.90

3.4 Morphology and chemical analysis of char residues

Next we analyzed char residues of EP and EP/HBPCP composites following cone calorimetry to elucidate the flame-retarding mechanisms. Digital photographs of residues from different angles (Fig. 7) show two distinct behaviors. Pure EP (a_2) leaves no coherent char layer and produces a grayish powder, whereas EP/HBPCP-1 (b_2) yields a darker powder residue, likely due to higher carbon content. As HBPCP loading increases, the char layer becomes increasingly continuous and intact, indicating HBPCP's role in promoting stable char formation during combustion (Li et al., 2014).

To further investigate HBPCP's flame-retarding mechanism, the microstructures of residual char surfaces of EP and EP/HBPCP composites were examined through scanning electron microscopy (SEM) following cone calorimetry. Additionally, energy-dispersive X-ray spectroscopy (EDS) was conducted to analyze the elemental composition and distribution on the char surfaces. SEM images revealed that pure EP and EP/HBPCP-1 lacked stable char layers. As HBPCP content increased, the char layers became progressively more continuous and compact with smaller pore sizes. Moreover, Table 5 shows that the content of phosphorus (P) and carbon (C) increased, contributing to the formation of a dense, integrated char layer.

In the FTIR spectra of residual chars (Fig. 9), absorption peaks at 3,436 cm^{-1} and 1,607 cm^{-1} were observed for both EP and EP/HBPCP-12.5, indicating hydroxyl, amino, and aromatic ring functionalities. In EP/HBPCP-12.5, new absorption peaks at 970 cm^{-1} and 1,110 cm^{-1} appeared, corresponding to P–O–P and P–O–C bonds, respectively (Yang et al., 2019). Furthermore, the C–H bending vibrational peak of methyl groups at 1,450 cm^{-1} disappeared. These results suggest that HBPCP's condensed-phase flame-retarding effect mainly originates from thermal degradation of the cyclotriphosphazene units. Phosphorus atoms act as links, forming thermally unstable crosslinked networks with methyl groups and aromatic rings. This network contributes to formation of a thermally stable, compact char layer that acts as a barrier between the polymer matrix and the external environment. By inhibiting heat, volatile gases, and oxygen exchange, this char layer effectively suppresses further combustion and enhances flame retardancy.

SEM images show that the residual char surfaces exhibit numerous pores, indicating gas migration from the EP matrix to the atmosphere during combustion. Cone calorimetry results further confirm that CO and CO_2 are present among the released gases. For the EP/HBPCP-10 composite, the N/P mass ratio decreased from 3.74 before combustion, to 0.39 after combustion (Table 5). This change suggests that a significant portion of nitrogen was released in gaseous form. During combustion, nitrogen can react with atmospheric oxygen to form non-combustible gases such as NO and NO_2, which dilute oxygen and flammable volatiles (Fang et al., 2020). These findings demonstrate that HBPCP contributes to composite flame retardancy through both condensed-phase and gas-phase mechanisms.

Unedited

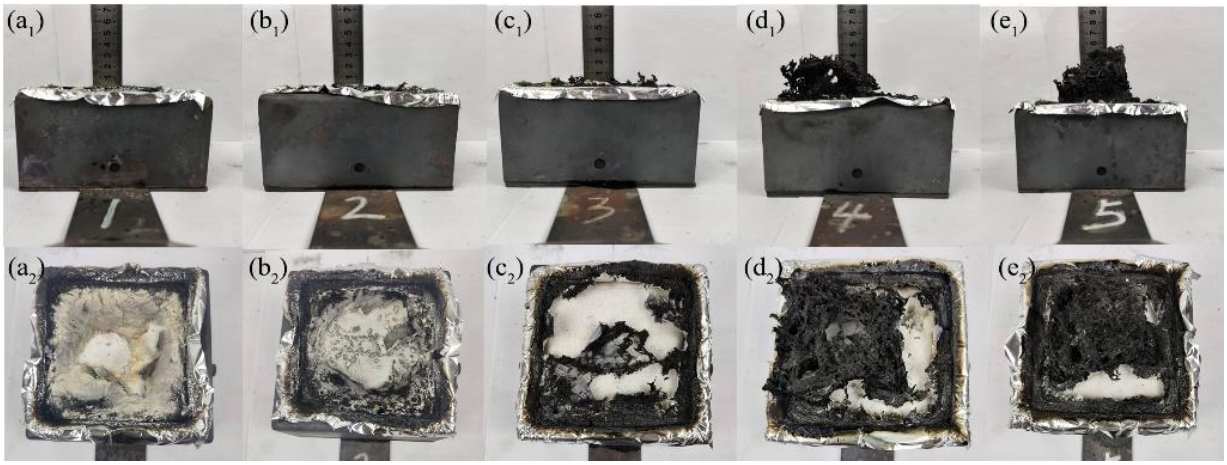

Fig. 7 Digital photographs of residual chars of EP (a_1, a_2), EP/HBPCP-1 (b_1, b_2), EP/HBPCP-5 (c_1, c_2), EP/HBPCP-10 (d_1, d_2) and EP/HBPCP-12.5 (e_1, e_2) from side and top views

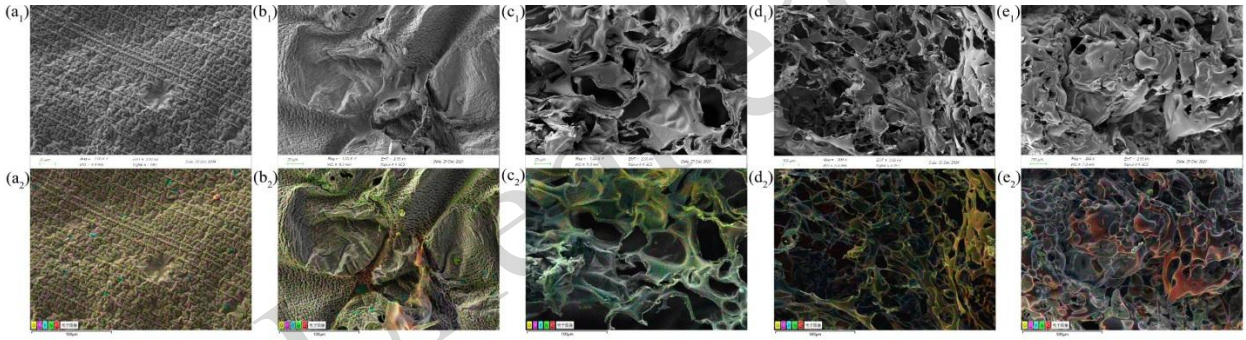

Fig. 8 SEM images and EDS-mapping images of residual chars of EP (a_1, a_2), EP/HBPCP-1 (b_1, b_2), EP/HBPCP-5(c_1, c_2), EP/HBPCP-10 (d_1, d_2), and EP/HBPCP-12.5 (e_1, e_2)

Table 5 The elemental distribution of residual char

Sample	Elemental distribution (wt.%)				
	C	N	O	P	S
EP	19.49	0.56	79.84	0	0.11
EP/HBPCP-1	23.95	0.77	64.67	10.56	0.06
EP/HBPCP-5	35.9	1.98	44.48	17.47	0.16
EP/HBPCP-10	59.37	3.59	27.59	9.28	0.26
EP/HBPCP-12.5	57.96	3.36	27.91	10.29	0.48

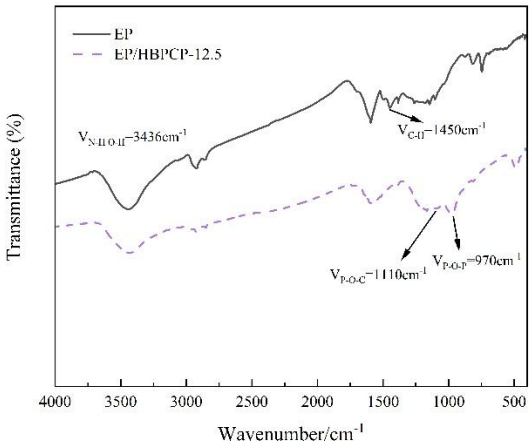

Fig. 9 FTIR spectrum of residual chars of EP and EP/HCPCP-12.5

3.5 Mechanical properties of the prepared EP and EP/HBPCP composites

We found that incorporating HBPCP into the epoxy resin improved the epoxy's mechanical strength. The mechanical properties increased initially with HBPCP content, but declined at higher loadings. The EP/HBPCP-5 composite exhibited the best mechanical performance, achieving a tensile strength of 37.72 MPa, which represents a 14.6% improvement over neat epoxy resin (32.91 MPa). This improvement is attributed to the uniform dispersion of HBPCP particles (≤75 μm) during processing. Due to their small particle size and high surface atom ratio, HBPCP particles readily form physical interactions with the epoxy matrix. First, the amide bond can form hydrogen bonds with the residual hydroxyl groups (-OH) and ether bonds (-O-) that remain after the curing of epoxy resin, consequently further enhancing the interface strength. Second, during tensile deformation, these particles act as anchors, hindering the initiation and propagation of microcracks. However, at higher HBPCP contents, stronger interparticle interactions hinder uniform dispersion in the resin. This leads to particle agglomeration, which adversely affects composite mechanical properties (Hu, 2019). Even at a high HBPCP loading of 12.5%, the composite's tensile strength and Young's modulus remained slightly higher than those of neat EP. Furthermore, the elongation at break remained nearly unchanged. Therefore, HBPCP addition not only preserves the mechanical integrity of epoxy resin, but enhances its overall performance.

Unedited

Table 6 Mechanical properties of the EP and EP/HBPCP composites

Sample	Tensile strength (MPa)	Elongation at break (%)	Young's modulus (GPa)
EP	32.91	6.52	0.13
EP/HBPCP-1	36.62	7.11	0.19
EP/HBPCP-5	37.73	6.55	0.32
EP/HBPCP-10	35.56	6.51	0.25
EP/HBPCP-12.5	33.29	6.44	0.17

3.6 Dielectric property

In electronic components, a low dielectric constant (D_k) and low dielectric loss factor (D_f) help reduce signal propagation delay and energy loss in high-speed signal transmission applications. Therefore, we chose to investigate the effect of varying HBPCP content on the dielectric properties of EP composites at high frequencies, as shown in Table 7. At 10 GHz, both the D_k and D_f values of the EP composites decreased with increasing HBPCP content. This phenomenon is mainly attributed to the increased free volume in the EP matrix as induced by incorporating HBPCP, which reduces the overall polarization and effectively decrease the D_k and D_f values of the EP/HBPCP composites (Hou et al., 2012).

Table 7 D_k and D_f of EP and EP/HBPCP composites

Sample	D_k	D_f
EP	3.26	0.0226
EP/HBPCP-1	3.24	0.0221
EP/HBPCP-5	3.14	0.0215
EP/HBPCP-10	3.12	0.0211
EP/HBPCP-12.5	3.10	0.0209

4 Conclusions

Hexa(p-methylbenzamidophenoxy)cyclotripho sphazene (HBPCP) has a molecular structure in

which amide linkages help connect rigid benzene rings, yielding exceptional thermal stability (41.82% char residue at 800 °C) and a high melting point (>300 °C). This ensures that HBPCP remains solid during epoxy resin (EP) processing at 185 °C, effectively preventing flame-retardant migration and ensuring uniform dispersion. In this study, EP/HBPCP composites were shown to exhibit superior flame retardancy: the limiting oxygen index (LOI) increased from 21.19% for pure EP to 27.13% for EP/HBPCP-12.5, and both EP/HBPCP-10 and EP/HBPCP-12.5 achieved a UL-94 V-0 rating. The peak heat release rate (PHRR) and total smoke production (TSP) were reduced by 49.2% and 41.8%, respectively, with suppressed CO and CO_2 emissions and no dripping behavior observed during combustion. Thermogravimetric and char residue analyses confirmed that HBPCP decomposes to generate phosphorus- and nitrogen-containing compounds, which quench free radicals in the gas phase and promote dense char formation in the condensed phase (with a 67% increase in char residue), demonstrating synergistic gas- and condensed-phase flame-retarding mechanisms. This work provides a straightforward strategy for developing high-performance, single-component flame-retardant systems. Since it acts as a matrix material for semiconductor encapsulation and laminates, dicyclopentadiene phenol epoxy resin's mechanical and dielectric properties are of paramount importance. Notably, the EP/HBPCP composites synthesized in this work were shown to have slightly enhanced mechanical strength and dielectric performance. At 10 GHz, the dielectric constant (D_k) decreased from 3.26 for pure EP to 3.10 for EP/HBPCP-12.5, which is attributed to the greater free volume within the epoxy matrix. Our findings establish a practical foundation for expanding the use of low-dielectric epoxy resins in high-frequency electronic devices and advanced microelectronic packaging.

Acknowledgments

This work is supported by the Key Deployment Project of the Chinese Academy of Sciences (ZDRW-CN-2023-6).

Author contributions

Yuyao JIA: conceptualization, methodology, experiment, data curation, and writing–original draft. Hao ZHU: experiment, data curation. Sheng ZOU: writing–review & editing. Wei BAI: funding acquisition, writing–review & editing. Qingyin WANG: funding acquisition, writing–review & editing.

Conflict of interest

Yuyao JIA, Hao ZHU, Sheng ZOU, Wei BAI, and Qingyin WANG declare that they have no conflict of interest.

References

Zhang Y, Song PA, Liu HZ, et al., 2016. Morphology, healing and mechanical performance of nanofibrillated cellulose reinforced poly(ε-caprolactone)/epoxy composites. *Composites Science and Technology*, 125:62-70. https://doi.org/10.1016/j.compscitech.2016.01.008

Xu ZG, Song PA, Zhang J, et al., 2018. Epoxy nanocomposites simultaneously strengthened and toughened by hybridization with graphene oxide and block ionomer. *Composites Science and Technology*, 168:363-370. https://doi.org/10.1016/j.compscitech.2018.10.020

Huo SQ, Liu ZT, Wang J, 2020. Thermal properties and flame retardancy of an intumescent flame-retarded epoxy system containing phosphaphenanthrene, triazine-trione and piperidine. *Journal of Thermal Analysis and Calorimetry*, 139(2):1099-1110. https://doi.org/10.1007/s10973-019-08467-3

Wang T, Wang J, Huo SQ, et al., 2016. Preparation and flame retardancy of DOPO–based epoxy resin containing bismaleimide. *High Performance Polymers*, 28(9):1090-1095. https://doi.org/10.1177/0954008316631591

Fu ZY, Ma ZR, Liu JH, et al., 2024. Phosphorus-containing active esters modified dicyclopentadiene epoxy resins with simultaneously improved flame retardancy, thermal stability, and dielectric properties. *Chemical Engineering Journal*, 482:148998. https://10.1016/J.CEJ.2024.148998

Lu JD, Zhang SL, Zhang LZ, et al., 2023. Preparation and properties of hollow glass microspheres/dicyclopentadiene phenol epoxy resin composite materials. *Materials (Basel, Switzerland)*, 16(10):3768. https://10.3390/MA16103768

Müller P, Schartel B, 2016. Melamine poly (metal phosphates) as flame retardant in epoxy resin: Performance, modes of action, and synergy. *Journal of Applied Polymer Science*, 133(24):43549. https://doi.org/10.1002/app.43549

Jin SL, Qian LJ, Qiu Y, et al., 2019. High-efficiency flame retardant behavior of bi-DOPO compound with hydroxyl group on epoxy resin. *Polymer Degradation and Stability*, 166:344-352. https://doi.org/10.1016/j.polymdegradstab.2019.06.024

Unedited

Müller P, Morys M, Sut A, et al., 2016. Melamine poly (zinc phosphate) as flame retardant in epoxy resin: Decomposition pathways, molecular mechanisms and morphology of fire residues. *Polymer Degradation and Stability*, 130:307-319. https://doi.org/10.1016/j.polymdegradstab.2016.06.023

Liu SH, Yu B, Feng YC, et al., 2019. Synthesis of a multifunctional bisphosphate and its flame retardant application in epoxy resin. *Polymer Degradation and Stability*,165:92-100. https://doi.org/10.1016/j.polymdegradstab.2019.04.022

Zhu ZM, Wang LX, Dong LP, 2019. Influence of a novel P/N-containing oligomer on flame retardancy and thermal degradation of intumescent flame-retardant epoxy resin. *Polymer Degradation and Stability*, 162:129-137. https://doi.org/10.1016/j.polymdegradstab.2019.02.021

Cheng HX, Guo JH, Ye Y, et al., 2024. Molecular design and properties of P-N-B co-intrinsic flame retardant thermosetting epoxy resin. *Journal of Applied Polymer Science*, 141(26):55575. https://doi.org/10.1002/app.55575

Wang W, He YS, Sun HW, et al., 2024. Synthesis of P/Si liquid flame retardant via the covalent modification and in-situ dispersion strategies for improving comprehensive performance of epoxy resin. *Composites Part A: Applied Science and Manufacturing*, 187:108468. https://doi.org/10.1016/j.compositesa.2024.108468

Yang YZ, Lin LM, Wang ZZ, 2025. Flame-retardant functionalized boron nitride for epoxy resin with excellent flame retardancy and enhanced thermal conductivity. *High Performance Polymers*, 37(4):252-267. https://doi.org/10.1177/09540083251319488

Li QL, Lei Y, Bi X, et al., 2025. Inspired by the tessellation of strawberry achenes on skin: Preparation of ZIF-67 derived multifunctional flame retardant through supramolecular assembly of cobalt alginate biopolymer in melamine-containing polyphosphazene skeleton. *Chemical Engineering Journal*, 506:160242. https://doi.org/10.1016/j.cej.2025.160242

Chen YJ, Shi Q, Liu JL, et al., 2025. Performance and mechanisms of P-N synergistic oligomeric flame retardants with different phosphorus oxidation states in epoxy resin. *Chemistryselect*, 10(21): e01534. https://doi.org/10.1002/slct.202501534

Wei YL, Bao LJ, Wu CC, et al., 2016. Characterization of anthropogenic impacts in a large urban center by examining the spatial distribution of halogenated flame retardants. *Environmental Pollution*, 215:187-194. https://doi.org/10.1016/j.envpol.2016.05.009

Huo SQ, Song PA, Yu B, et al., 2021. Phosphorus-containing flame retardant epoxy thermosets: Recent advances and future perspectives. *Progress in Polymer Science*, 114:101366. https://doi.org/10.1016/j.progpolymsci.2021.101366

Liu JH, He ZJ, Wu GH, et al., 2020. Synthesis of a novel nonflammable eugenol-based phosphazene epoxy resin with unique burned intumescent char. *Chemical Engineering Journal*, 390:124620. https://doi.org/10.1016/j.cej.2020.124620

Bose S, Mukherjee M, Das CK, et al., 2010. Effect of polyphosphazene elastomer on the compatibility and properties of PES/TLCP composites. *Polymer Composites*, 31(3):543-552. https://doi.org/10.1002/pc.20840

Khalidah USN, Zuhair J, Hilmey MMZ, 2021. A Review on Synthesis, Structural, Flame Retardancy and Dielectric Properties of Hexasubstituted Cyclotriphosphazene. *Polymers*, 13(17):2916. https://doi.org/10.3390/polym13172916

Jiang JW, 2022. Flame retardancy of epoxy resin with metal-organic framework hybrid and hexaphenoxycyclotriphosphazene. MS Thesis, Zhejiang University, Hangzhou, China (in Chinese).

Tang AB, Huang J, Shao YT, et al., 2010. Synthesis of Hexaphenoxycyclotriphosphazene and Its Application in Laminate. *Chinese Journal of Applied Chemistry*, 27(4):404-408 (in Chinese). https://doi.org/10.3724/SP.J.1095.2010.90390

SHIN YJ, HAM YR, KIM SH, et al., 2009. Application of cyclophosphazene derivatives as flame retardants for ABS. *Journal of Industrial and Engineering Chemistry*, 16(3):364-367. https://10.1016/j.jiec.2009.08.001

ATIKA NW, ZUHAIR J., 2023. Synthesis and mechanical property of hexasubstituted cyclotriphosphazene derivatives attached to hydrazine-bridge linkage with high fire retardancy. *Journal of Molecular Structure*, 1284(15):135330. https://doi.org/10.1016/j.molstruc.2023.135330

Chen BX, Li J, Wang M, et al., 2024. Effect of post-polymerization on the crystallization and melting behavior of poly(butylene terephthalate). *Polymer*, 294:126675. https://doi.org/10.1016/j.polymer.2024.126675

Wang, CH, Hu F, Yang KJ, et al., 2015. Synthesis and properties of star-branched nylon 6 with hexafunctional cyclotriphosphazene core. *RSC Advances*, 5(107):88382-88391. https://doi.org/10.1039/C5RA15598C

Wang SM, Zhao C, Zhang X, et al., 2019. Clickable coupling of carboxylic acids and amines at room temperature mediated by SO_2F_2: A significant breakthrough for the construction of amides and peptide linkages. *Organic & Biomolecular Chemistry*, 17(16):4087-4101. https://doi.org/10.1039/C9OB00699K

Cheng JW, Wang J, Yang S, et al., 2019. Benzimidazolyl-substituted cyclotriphosphazene derivative as latent flame-retardant curing agent for one-component epoxy resin system with excellent

Unedited

comprehensive performance. *Composites Part B*, 177:107440. https://doi.org/10.1016/j.compositesb.2019.107440

Jiang JW, Huo SQ, Zheng Y, et al., 2021. A novel synergistic flame retardant of hexaphenoxycyclotriphosphazene for epoxy resin. *Polymers*, 13(21):3648. https://doi.org/10.3390/polym13213648

Nabipour H, Wang X, Rahman MZ, et al., 2022. Improvement of the flame retardant and thermomechanical properties of epoxy resins by a vanillin-derived cyclotriphosphazene-cored triazole compound. *Polymer Degradation and Stability*, 204:110088. https://doi.org/10.1016/j.polymdegradstab.2022.110088

Jiang WZ, Hao JW, Han ZD, 2012. Study on the thermal degradation of mixtures of ammonium polyphosphate and a novel caged bicyclic phosphate and their flame retardant effect in polypropylene. *Polymer Degradation and Stability*, 97(4):632-637. https://doi.org/10.1016/j.polymdegradstab.2012.01.001

Sun N, Qian LJ, Xu GZ, et al., 2014. Pyrolysis of hexa-phenoxyl-cyclophosphazene and its flame retardant mechanism to epoxy resin. *Scientia Sinica(Chimica)*, 44(7):1195-1202 (in Chinese). https://doi.org/10.1360/N032013-00062

Seraji SM, Gan HL, Swan SR, et al., 2021. Phosphazene as an effective flame retardant for rapid curing epoxy resins. *Reactive and Functional Polymers*, 164:104910. https://doi.org/10.1016/j.reactfunctpolym.2021.104910

Kurta A, Nicolasb D, Guillermo BP, et al., 2013. Cyanide poisoning by fire smoke inhalation: a European expert consensus. *European journal of emergency medicine*, 20(1):2-9. https://doi.org/10.1097/MEJ.0b013e328357170b

Li Z, Lira SIM, Zhang L, et al., 2018. Bio-inspired engineering of boron nitride with iron-derived nanocatalyst toward enhanced fire retardancy of epoxy resin. *Polymer Degradation and Stability*, 157:119-130. https://doi.org/10.1016/j.polymdegradstab.2018.10.005

Yuan BH, Sun YR, Chen XF, et al., 2018. Poorly-/well-dispersed graphene: abnormal influence on flammability and fire behavior of intumescent flame retardant. *Composites Part A: Applied Science and Manufacturing*, 109:345-354. https://doi.org/10.1016/j.compositesa.2018.03.022

Wang PJ, Liao DJ, Hu XP, et al., 2019. Facile fabrication of biobased P-N-C-containing nano-layered hybrid: preparation, growth mechanism and its efficient fire retardancy in epoxy. *Polymer Degradation and Stability*, 159:153-162. https://doi.org/10.1016/j.polymdegradstab.2018.11.024

Li JW, Pan F, Xu H, et al., 2014. The flame-retardancy and anti-dripping properties of novel poly(ethylene terephalate)/cyclotriphosphazene/silicone composites. *Polymer Degradation and Stability*, 110:268-277. https://doi.org/10.1016/j.polymdegradstab.2014.08.027

Yang G, Wu WH, Wang YH, et al., 2019. Synthesis of a novel phosphazene-based flame retardant with active amine groups and its application in reducing the fire hazard of Epoxy Resin. *Journal of Hazardous Materials*, 366:78-87. https://doi.org/10.1016/j.jhazmat.2018.11.093

Fang YZ, Miao JS, Yang XW, et al., 2020. Fabrication of polyphosphazene covalent triazine polymer with excellent flame retardancy and smoke suppression for epoxy resin. *Chemical Engineering Journal*, 385:123830. https://doi.org/10.1016/j.cej.2019.123830

Hu GQ, 2019. Study on properties of epoxy resin-based carbon fiber composites modified by inorganic particles. MS Thesis, Nanchang University, Nanchang, China (in Chinese).

Hou CC, Hung TL, Ching HL, 2012. Benzoxazine-based phosphinated bisphenols and their application in preparing flame-retardant, low dielectric cyanate ester thermosets. *Polymer chemistry*, 3(4):970-978. https://doi.org/10.1039/C2PY00528J

Unedited

中文概要

题　　目：一种新型磷腈阻燃剂在双环戊二烯苯酚型环氧树脂中的应用

作　　者：贾雨耀[1,2]，朱昊[1,2]，邹胜[1]，白威[1]，王庆印[1]

机　　构：[1]中国科学院成都有机化学研究所，中国成都，310027；[2]中国科学院大学，中国北京，101400

目　　的：以制备层压板为例，环氧树脂需在高温高压环境下进行固化。以熔点为 114 ℃ 的六苯氧基环三磷腈为例。在 185 ℃ 高温下进行热压，随着固化过程的进行环氧树脂粘度越来越大，液态的六苯氧基环三磷腈反而会被压至基材表面，从而造成环氧树脂内部组分分布不均，从而使得固化后的环氧树脂力学性能下降。使用本文所要制备一种高热稳定性的磷腈材料以提高其加工性能。

创新点：在六苯氧基环三磷腈的基础上以酰胺键为连接点，制备了磷腈衍生物六对甲基苯酰胺苯氧基环三磷腈（HBPCP），由于其分子量增大以及酰胺键的高极性，其具有高熔点和高热稳定性。分两步引入苯环结构，在一定程度上克服了空间位阻效应，提高了目标产物的产率且几乎无其他副产物。

方　　法：通过核磁和红外对 HBPCP 进行结构测定，使用 TGA 和 DSC 对 HBPCP 和 EP/HBPCP 复合材料进行了热稳定性的测试。使用垂直燃烧测试、极限氧指数和锥形量热测试对其进行了阻燃性能测试。使用 SEM、红外进行了残炭的构成分析。使用万能万能

拉伸测试仪进行力学性能测试。采用 P937XA USB 矢量网络分析仪分析测试介电常数和介质损耗，10GHz。

结　论：对甲基苯酰胺苯氧基环三磷腈（HBPCP）的分子结构由酰胺键连接着坚固的苯环构成，具有极高的热稳定性(在 800 °C 时残余碳含量为 41.82%）和较高的熔点（>300 °C）。这确保了在 185 °C 的环氧树脂（EP）加工过程中，HBPCP 保持固态，有效地防止了阻燃剂的迁移，并确保了均匀分散。EP/HBPCP 复合材料表现出卓越的阻燃性能：纯 EP 的极限氧指数（LOI）从 21.19% 提高到 EP/HBPCP-12.5 的 27.13%，而 EP/HBPCP-10 和 EP/HBPCP-12.5 都达到了 UL-94 V-0 等级。峰值热释放速率（PHRR）和总烟雾产生量（TSP）分别降低了 49.2% 和 41.8%，同时减少 CO 和 CO_2 的排放，并且在燃烧过程中没有滴落现象。热重分析和残余物分析证实，HBPCP 分解生成含磷和氮的化合物，这些化合物能抑制气相中的自由基并促进凝聚相中致密炭的形成（残余物增加 67%），展示了气相和凝聚相协同的阻燃机制。这项研究提供了一种开发高性能单组分阻燃系统的简单方法。作为半导体封装和层压板的关键基质材料，二环戊二烯酚环氧树脂的机械性能和介电性能同样至关重要。EP/HBPCP 复合材料不仅保持了原有的机械强度和介电性能，还略有提升。在 10GHz 频率下，介电常数（D_k）从纯 EP 的 3.26 降至 EP/HBPCP-12.5 的 3.10，这归因于环氧基质内自由体积的增加。这些进展为在高频电子设备和先进微电子封装中扩大低介电环氧树脂的应用奠定了实用的基础。

关键词：环三磷腈衍生物；阻燃剂；环氧树脂；高热稳定性；低介电；通讯材料

Unedited